Design of Compact Dual-Polarized 1.2–10 GHz Eleven Feed for Decade Bandwidth Radio Telescopes

Jian Yang, *Senior Member, IEEE*, Miroslav Pantaleev, Per-Simon Kildal, *Fellow, IEEE*, and Leif Helldner

***Abstract*—The Eleven antenna is a log-periodic folded-dipole-pair array with two unique radiation characteristics: a constant beamwidth and a fixed phase center location over a decade bandwidth. This paper presents a new compact design of a 1.2–10 GHz Eleven antenna, as a feed for reflector antennas by re-arranging the geometry of the outermost elements of the antenna. Due to the compact size, it is possible to put the whole feed system inside a compact cryostat and cool it down to cryogenic temperatures, in order to reduce the system noise temperature in radio telescope applications. The new compact Eleven feed has only a 40% volume of the original standard Eleven feed with a very similar performance. This reduces the capacity requirement for the cryogenic cooling system significantly and therefore the power consumption for future radio telescopes, such as the square kilometer array (SKA). The concept behind this compact design is analyzed in the paper. Simulations and measurements presented here have verified the design.**

***Index Terms*—Compact antenna, Eleven antenna, log-periodic array, low noise temperature, ultra-wideband antenna.**

I. Introduction

RADIO telescopes with large decade-bandwidth have many advantages. They provide super-sensitivity which makes extremely low temperatures in the universe measurable [1]. Their simultaneous multi-channel observations in frequency domain offer possibilities to observe large number of spectral lines, and therefore increase both the speed and accuracy of the observation (for example in the geodetic Very Long Base Interferometry experiments) [2]. Ultra wide bandwidth allows pulse observation in time domain, which is critical in applications such as the observation of different forms of solar activity [3]. Many proposals for future radio telescopes require such wideband systems, for example, 1.2–10 GHz mid-frequency dish array of the SKA (Square Kilometer Array) [4] and 2–13 GHz reflectors for VLBI2010 (Very Long Baseline Interferometry 2010) [2].

There are several reflector feed technologies for decade-bandwidth radio telescopes under development, such as the Eleven feed, the quadridge horn [5], the improved quadruple-ridged flared horn [6], the sinuous feed [7] and the quasi self-complementary antenna [8]. The main drawback of the quadridge horn as a feed for reflectors is that its beamwidth and phase center location vary with frequency, which leads to a low aperture efficiency; see the comparison of the radiation performance between the Eleven feed and the quadridge horn in [9]. The improved quadruple-ridged flared horn has much more constant beamwidth compared to the original quadridge horn but the phase center varies with frequency. Both the sinuous feed and the quasi self-complementary antenna are non-planer wideband log-periodic dual polarization antennas. The polarization angle of the two antennas varies with frequency and no hardware has yet been realized above 4 GHz.

The Eleven feed is a decade-bandwidth log-periodic dual-dipole array antenna. It has two unique radiation characteristics: a constant beamwidth and a fixed phase center location over a decade bandwidth. In addition, it has a reflection coefficient below -10 dB over nearly a decade bandwidth, low cross polarization level, and a simple geometry with a low profile. Therefore, the Eleven antenna is a very promising candidate for decade-bandwidth reflector feed in future radio telescopes, demonstrated in [10] and [13].

Radio telescope applications require extremely low system noise temperatures, such as the goal of below 35 K in the mid-frequency band (1–10 GHz) SKA project. For a frequency range of a few GHz, a feed system consisting of corrugated feed horn, combined with cryogenically cooled LNAs, usually has noise temperature in the order of 20K over an octave bandwidth. It is therefore critical to integrate and cryogenically cool LNAs and feeds in both VLBI2010 and mid-frequency SKA systems, to be competitive with the corrugated feed horns. In addition, the feed and its cryogenic chamber (cryostat) should be sufficiently compact in order to fit in the focal area of the reflector, with minimum blockage of the reflector aperture. Consequently, size and cryogenic cooling concerns (such as out-gassing, heat conductance and thermally-induced mechanical stress) play important roles in the design of decade-bandwidth feeds for VLBI2010 and SKA radio telescopes.

In addition to applications in radio telescopes, the Eleven antenna can be used in other areas, for example, in satellite communication systems as terminals with mono-pulse tracking functions [14], as an ultra-wideband MIMO antenna for MIMO systems [15], [16], and as a digital television antenna [17]. The Eleven antenna can also be combined with a centrally located high frequency horn to make a dual band feed for monitoring antennas in satellite communication systems [18].

The purpose of this work is to design a compact 1.2–10 GHz Eleven feed for the SKA project, which should fit into the same

Manuscript received June 28, 2011; revised October 07, 2011; accepted November 24, 2011. Date of publication March 02, 2012; date of current version May 01, 2012. This work was supported in part by The Swedish Foundation for Strategic Research (SSF) within the Strategic Research Center Charmant.

J. Yang and P.-S. Kildal are with the Dept of Signals and Systems, Chalmers University of Technology, S-41296 Gothenburg, Sweden (e-mail: jian.yang, per-simon.kildal@chalmers.se).

M. Pantaleev and L. Helldner are with Onsala Space Observatory, Chalmers University of Technology, S-41296 Gothenburg, Sweden (e-mail: miroslav.pantaleev@chalmers.se; leif.helldner@chalmers.se).

Color versions of one or more of the figures in this paper are available online at http://ieeexplore.ieee.org.

Digital Object Identifier 10.1109/TAP.2012.2189732

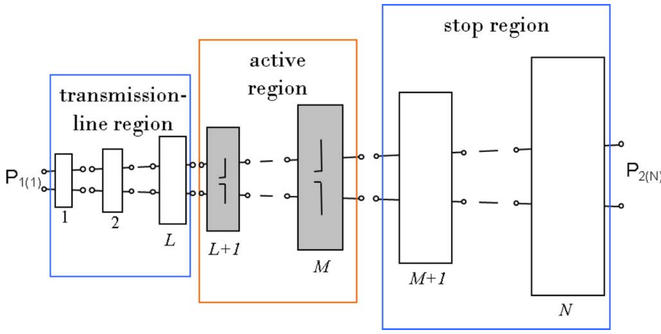

Fig. 1. N-element cascaded log-periodic array, where the symbol of dipole represents radiation.

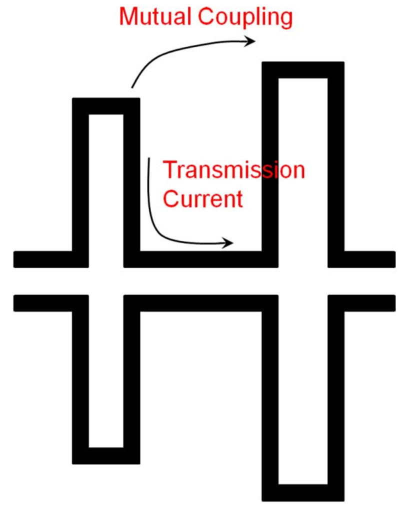

Fig. 2. Mutual couplings and transmission current.

cryostat for the 2–13 GHz Eleven feed for VLBI2010 [13], instead of using a nearly double-sized cryostat due to the frequency band. With the compact feed, the energy consumption for cryogenic cooling of thousands of feeds in the SKA can be reduced significantly. Therefore, this work is important to fulfill the very strict requirements for minimizing the power consumption in the SKA [19].

The compact design is obtained by folding down the outermost three non-radiating elements in the antenna. In Section II, we describe the theory on compacting a general log-periodic array. Two alternative compact designs for the 1.2–10 GHz Eleven feed are discussed in Section III. Optimization procedure used in the design is described in Section V. Then, the measured and simulated results are presented to verify the compact design in Section VI.

II. Theory on Compacting Log-Periodic Array

In general, in order to make a log-periodic array (LPA) antenna function properly over a certain operating frequency band, the LPA should be constructed in such a way that there always exist three regions (transmission-line, active and stop) over the operating frequency band. The definitions of the three regions can be found in [1] and we describe them in a stricter way for the sake of analysis here. It is also assumed in this work that the excitation (feeding) port is at the input port of the smallest radiation element in the LPA, as shown in Fig. 1, which is also the case for the most LPAs in practice.

1) The Transmission-Line-State Region: The transmission-line-state region (referred to as the transmission-line region in the paper) in a LPA at a frequency f is the region where the elements do not radiate. This is because the size of the elements is much smaller than the wavelength at f, and therefore they function as a transmission line. Shown in Fig. 1, the elements from 1 to L are in the transmission-line region.

2) The Active-Radiating-State Region: The active-radiating-state region (active region) in a LPA at a frequency f is the region where the elements radiate. Shown in Fig. 1, the elements from $L+1$ to M radiate.

3) The Stop-State Region: The stop-state region (stop region) in a LPA at a frequency f is the region after the active region, where the elements do not radiate, even though the size of the elements is comparable to the wavelength at the frequency f. Non-radiation in the stop region is due to that the current on these elements vanishes. This current vanishing is the result of the following fact: the current passed through the previous element and the current induced by mutual couplings from the active radiation elements via free space (Fig. 2) are of the same amplitude and 180° out of phase [20], [21].

The purpose of having a stop region in a LPA is twofold: keep the log-periodic geometry of the array for the operating frequency band, in order to have constant radiation performance for the band [21], and properly terminate the LPA. Since there are no currents on the elements in the stop region, the termination of the last element can be either shorted, open or by other ways. For example, the last dipole of the Eleven feed is shorted to the ground plane in order to have a good thermal conductivity in this work.

Having a stop region however makes the size of the whole LPA antenna large, because the elements in the stop region are large due to the periodicity. In this work, for example, we need three elements in the stop region for the frequency of 1.2 GHz, and the volume of the antenna including these three elements is therefore almost 7 times of the volume of the feed without the three elements. Thus, re-arrangement of the elements in the stop region may lead to a compact solution to a LPA antenna.

Based on the above analysis, the re-arrangement of the elements in the stop region should be carried out under the following constraints: these elements should not radiate (kept as non-radiating elements), and the effect on the radiating elements on both radiation performance and reflection coefficient should be minimum. This implies that the mutual couplings and the current transmissions among these elements should be kept as close to the original one as possible, see Fig. 2. Obviously it is too complicated to find a geometry fulfilling the constraints by an analytical method. Therefore, numerical optimization is applied to this task.

III. Two Alternative Compact Designs

In principle, there could be many possible alternatives of compact geometries which satisfy the requirement discussed above. Two of them have been investigated: the curve bend and the 90° bend. The reason that the two alternatives are presented in the paper is that though the 90° bend is chosen for the

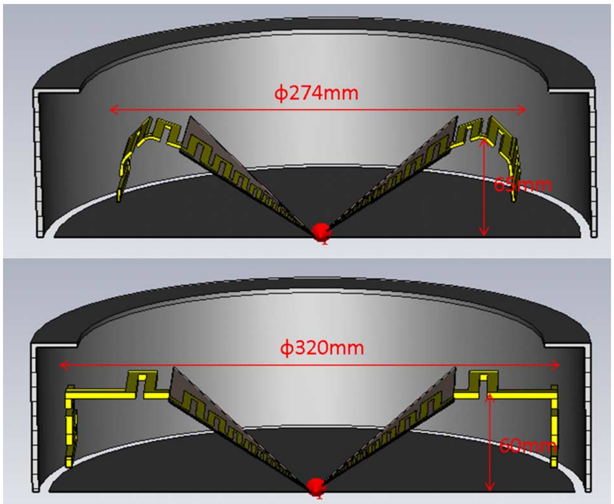

Fig. 3. Two alternative compact designs: the curve bent folding (up) and the 90° bend folding (down). In the figure a cut through half of the geometry of the whole array for single polarization is used for the sake of clarity. (color codes: gray—Aluminum, yellow—copper, gray pink—Rogers TMM3).

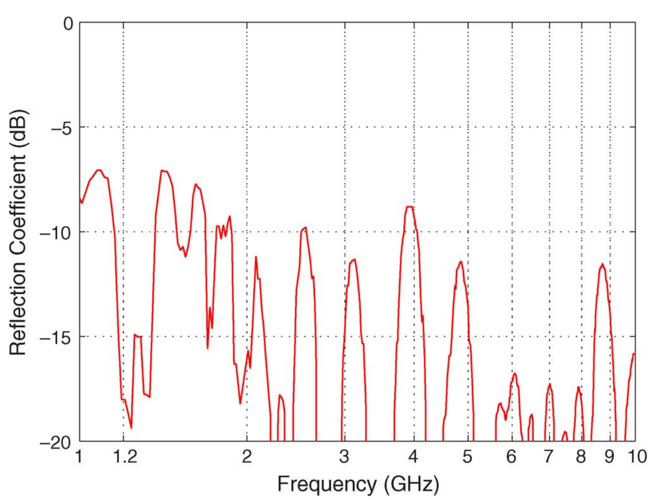

Fig. 4. Simulated reflection coefficient of a curve bend folding solution.

prototype in the work due to the low manufacture cost, it is still open for the curved-bent solution when the mass production is the case in the future.

It should be noted that in the compact designs, a simple metal cylinder, without much details which we believe have not much effect, is always included to emulate the actual cryostat used in the project, since the cryostat has a strong impact on the performance at the low frequency end of the band.

A. Curve Bend

Fig. 3 (up) shows the 3D model created in CST Microwave Studio [22] of the curved-bent solution to compact design: each element in the stop band is folded down gradually. Note that in order to present the re-arrangements clearly, we show a cut through half of the geometry of the whole array for a single polarization. The advantage of this solution is that the geometrical change in the stop region is smooth, and consequently, this compact design should have a smooth performance (without rapid change) at the low end of the band. Fig. 4 shows a preliminary

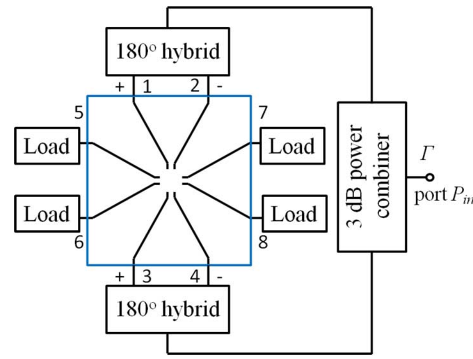

Fig. 5. Ideal feeding network consisting of two hybrids and one 3-dB power divider for the Eleven feed.

result of the simulated reflection coefficient of this type, where the input port is at the port of the first dipole, with a reference impedance of 200 Ohms as shown by the red arrow in Fig. 3.

The volume reduction by the curved-bent solution is quite significant. Compared to the standard unfolded 1.2–10 GHz Eleven feed, shown in Fig. 8, this compact feed has a volume of only 32% of that of the standard one. However, the manufacture cost, specially for one prototype, is quite high, due to the complexity of this geometrical re-arrangement (a mold is needed for pressing the elements into a specific curve). Therefore, this alternative of compact geometry has not been manufactured for verification and further investigation in this work, but is left open to compact solution for future mass production.

B. 90° Bend

Fig. 3 (down) shows the CST modeling of the 90°-bent solution: the elements are bent to the horizontal and then to the vertical. The main advantages of this structure are the much lower manufacture cost compared to the curve bend and the better mechanical stability. Thus, this alternative is chosen to go through the whole optimization procedure and one prototype has been manufactured in the work, which is referred to as the folded compact Eleven feed below. It is also obvious that the geometrical change of this solution is quite dramatic, and the performance of this alternative may therefore have some dramatic change at the low end of the band. Consequently, a heave optimization is required.

IV. Characterizations of the Eleven Feed for Optimization

The optimization procedure is based on the following characterizations of the Eleven feed.

A. Reflection Coefficient

The center puck circuit board for the 1.2–10 GHz Eleven feed used in this work is the same one for 2–13 Eleven feed in [13], which is a 8-port circuit shown in Fig. 10. With the reference to Figs. 5 and 10, the reflection coefficient Γ is defined as

$$\Gamma = S_{11} - S_{12} + S_{13} - S_{14}, \quad (1)$$

while ports 5, 6, 7 and 8 for the other polarization are terminated by loads. The formula in (1) corresponds to the reflection coefficient at port P_{in}, using an ideal feeding network consisting of two ideal 180° hybrids (baluns) and one ideal 3-dB power combiner, as shown in Fig. 5, to combine the signals received by the antenna petals.

B. Aperture Efficiency

The aperture efficiency of the Eleven feed can be calculated by several sub-efficiencies [23] as

$$e_{ap} = e_{sp} e_{BOR_1} e_{pol} e_{ill} e_{\phi} \tag{2}$$

where e_{sp} is the spillover efficiency with the subtended angle θ_0; e_{BOR_1} is the BOR_1 (body of revolution) efficiency within θ_0; e_{pol}, e_{ill} and e_{ϕ} are the polarization efficiency, the illumination efficiency and the phase efficiency, all of the BOR_1 component and within θ_0, respectively. Note that e_{sp} is evaluated on the total radiation function, not only on its BOR_1 component.

C. Co- and Cross-Polar Radiation Pattern

Although the Eleven antenna is not a BOR (body of revolution) structure antenna, it has a high BOR_1 efficiency. Therefore, the co- and cross-polar radiation functions of the BOR_1 component are mainly concerned, which can be written as [23]

$$\begin{aligned} G_{co}(\theta,\varphi) &= G_{co45}(\theta) - G_{xp45}(\theta)cos(2\varphi) \\ G_{xp}(\theta,\varphi) &= G_{xp45}(\theta)sin(2\varphi). \end{aligned} \tag{3}$$

Thus, the radiation characterization of the BOR_1 component of the Eleven feed is defined by the co- and cross-polar radiation functions in 45° plane: $G_{co45}(\theta)$ and $G_{xp45}(\theta)$.

V. Optimization Scheme—Genetic Algorithm

A global optimization scheme—the Genetic Algorithm (GA) has been applied to optimize the configuration of the 90° bent folding structure, together with using CST MS [22] as the electromagnetic solver. The GA scheme used here is similar to that in [24].

The 1.2–10 GHz Eleven antenna is designed with four petals for dual polarizations; on each of them the log-periodic array consists of 17 cascaded folded dipoles. The innermost 14 folded dipoles on each petal have the same geometry on Rogers TMM3 substrate as those used in the 2–13 GHz Eleven feed presented in [13] and [25]. The reason for this is that we want to use the same center puck, feeding network and ports for both the 1.2–10 GHz and 2–13 GHz Eleven feeds. The operating frequency for the 14th element is 1 GHz. The rest outermost 3 elements are in the stop region for the frequency band of 1.2–10 GHz.

The optimization is carried out on dimensions of the outermost three dipoles with a metal plate connected to the ground plane, see Fig. 6. Since the outermost three dipoles affect the performance of the Eleven feed mainly at low frequencies, the optimization is performed for the frequency range of 1–3 GHz, which makes the whole feed (including the cryostat) not very large in terms of wavelength (1.4 million meshcells with 20 lines per wavelength at 3 GHz modeled in CST MWS).

The goal of the optimization is to minimize the reflection coefficient and keep a good radiation performance. The genes in this GA optimization can be expressed as

$$gene = \{k_{15}, k_{16}, k_{17}, L_{15}, L_{16}, L_{17}, L, D, H_1, H_2\}$$

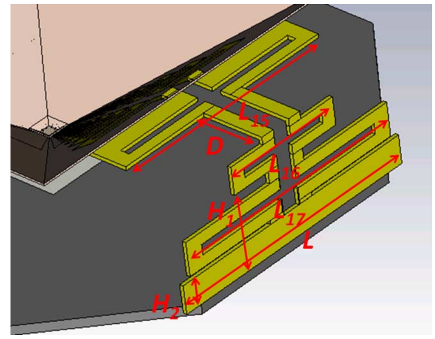

Fig. 6. Definition of dimensions of the outermost three dipoles in the compact design of 1.2–10 GHz Eleven antenna for optimization.

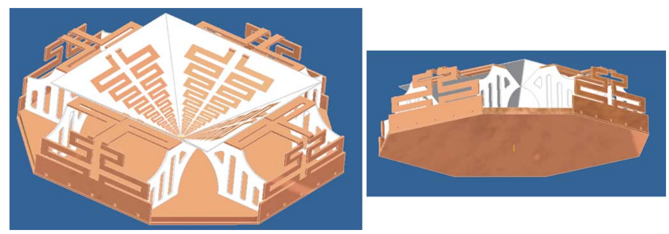

Fig. 7. Final geometry of the 1.2–10 GHz Eleven feed after optimization.

where k_{15}, k_{16}, and k_{17} are the scaling factors for dipoles 15, 16, and 17, respectively, and other dimensions are defined in Fig. 6. Floating-point data are used to express the chromosome.

The first generation is created randomly with a population of 50 individuals. Then, an elite group of 10 individuals with the best genes is selected and two-point crossover is applied among the elite individuals in the group to create genes for the next generation. A roulette-wheel selection is used to choose the genes from the remaining non-elite population, and the selected genes are over-crossed to create the genes for the rest of the population in the next generation. If the population of the next generation is fewer than 50 due to the mechanical constraints, mutation and random creation are used to create more genes. In this work, after 5 generations, the best genes become convergence.

Fig. 7 shows a mechanical drawing of the final optimized geometry of the antenna. It can be seen that the outermost three dipoles are not periodically scaled any more. It is also noticed that though dipole 16 is shorter than it was before the re-arrangement, it is non-radiating element in the stop region. As it is explained in Section III-B, the 90° bend compact design makes the geometry change dramatically, and consequently leads to a dramatic change of the size and location of the dipoles, in order to fulfill the condition for the stop region—the current vanishes.

A comparison between the folded compact Eleven feed and the standard unfolded one has been carried out in simulation. The geometry of these two feeds is shown in Fig. 8. It can be seen that the compact design has only 40% volume of the standard one. Therefore, the same compact cryostat for 2–13 GHz Eleven feed can be used for the 1.2–10 GHz feed. Fig. 9 shows the comparison of the simulated performance (with a 0.1 GHz frequency interval) between the two feeds, where the aperture efficiency is calculated for a reflector with a subtended angle of $2 \times 60°$ and without the blockage efficiency included. It can be

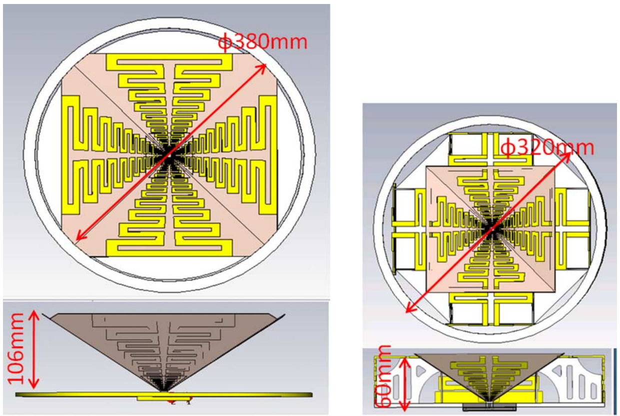

Fig. 8. Compact 1.2–10 GHz Eleven feed has only 40% volume of the standard one. (a) Standard unfolded; (b) folded compact.

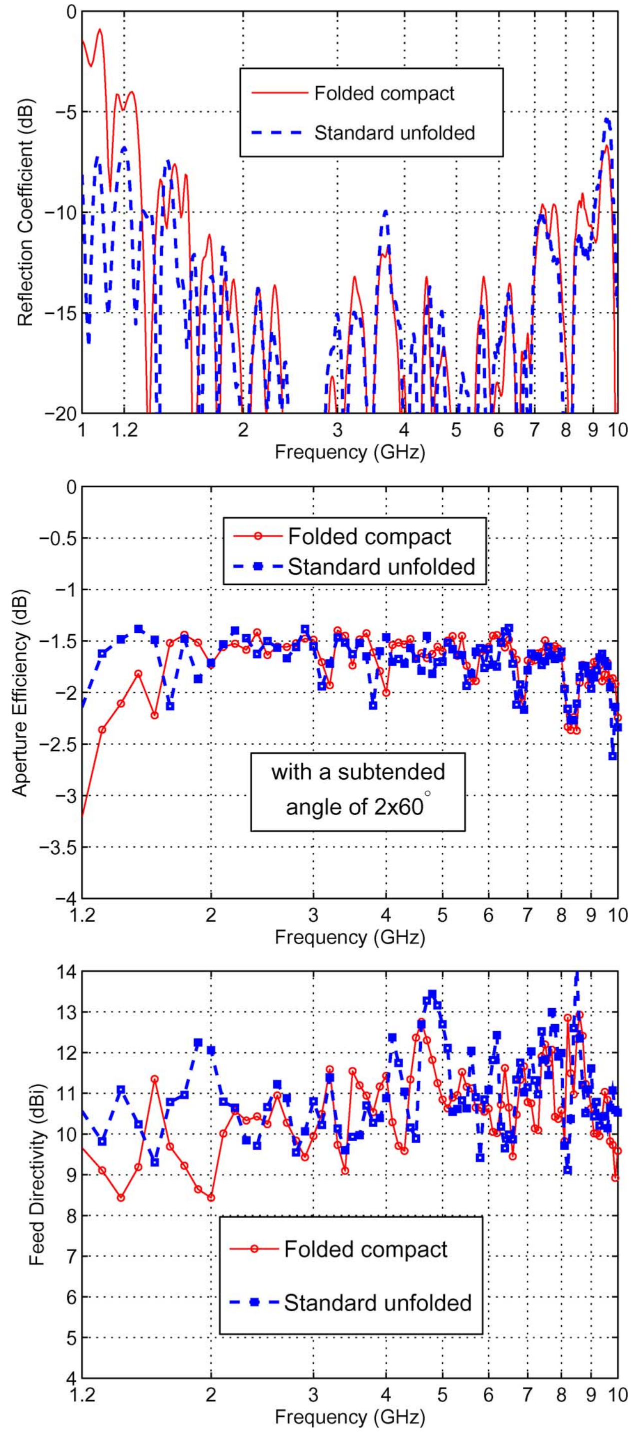

Fig. 9. Comparison of simulated performance between the folded compact antenna and the standard unfolded one: the reflection coefficient (up), the aperture efficiency (middle) and the directivity (low).

concluded that the compact Eleven feed has a very similar performance to that of the standard one over 1.2–10 GHz, though the standard one has better performance at 1.2 GHz. It is also noticed that the reflection coefficient of the compact antenna changes rapidly around 1.2 GHz.

VI. Simulated and Measured Results

The modeling and the manufactured hardware of the compact 1.2–10 GHz Eleven feed with a cylinder emulating the cryostat are shown in Fig. 10.

All simulated results presented here are obtained by using CST MWS [22], which includes the center puck circuit board, as shown in Fig. 10(a). The simulated reflection coefficient is at the input port (port 1) with a port impedance (reference impedance) of 50 Ohms. Note that we have used two symmetry planes in the simulation: the PEC (perfect electric conductor) plane and the PMC (perfect magnetic conductor) plane. By doing so, the size of the problem is reduced to the quarter of the original one, and the reflection coefficient at port 1 is equivalent to that determined by (1) when the whole geometry is included in simulation.

The reflection coefficient is measured at ports 1–4 with 50 Ohm SMA connectors, shown in Fig. 10(b). A feeding network, including two 180° hybrids and one 3-dB power divider, is used in the measurement. The calibration is done at the output ports of the feeding network (these output ports will be connected to ports 1–4 of the antenna) so the effect (ohmic loss, etc.) of the feeding network has been calibrated out.

The complex far-field functions are measured in the anechoic chamber at the Antenna Group at Chalmers University of Technology, in terms of co- and cross-polar components in Ludwig's third definition, with 2 degree interval for both θ and φ and 0.1 GHz frequency interval.

The measured and simulated reflection coefficients of the Eleven feed are shown in Fig. 11. It can be observed that the measured reflection coefficient is below -10 dB over the most part of the 1.2–10 GHz band, and there are only a few peaks above the -10 dB level, and all of them are below -8 dB.

Fig. 12 shows the measured co- and cross-polar radiation patterns and the BOR_1 components in 45° plane. It can be seen that the beamwidth of the pattern is nearly constant over the frequency band, and the cross-polarization level is below about -15 dB.

Fig. 13 presents the calculated sub-efficiencies for the 1.2–10 GHz Eleven feed when it illuminates a parabolic reflector with a subtended angle of $2 \times 60°$, both based on the simulated and measured complex far-field functions. The reason that we choose this subtended angle is that this value

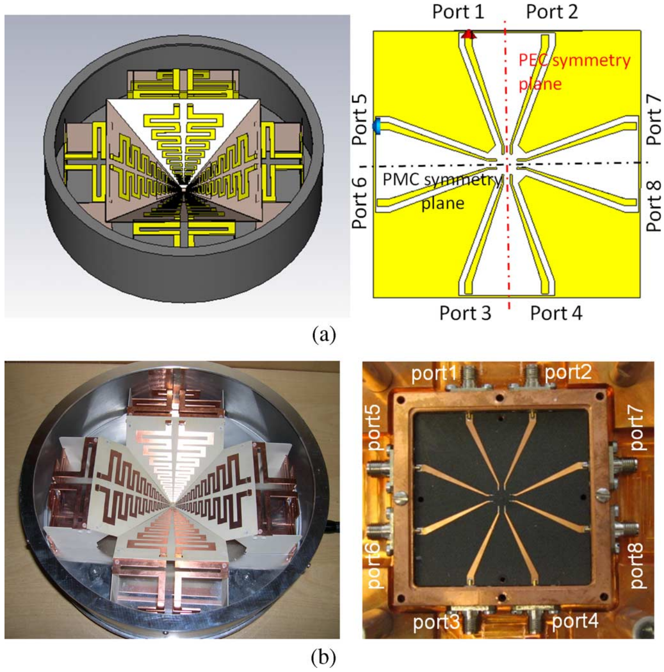

Fig. 10. Model in CST MWS and Photo of the manufactured 1.2–10 GHz Eleven feed (left), and the 8-port center puck circuit board at the rear side of the ground plane (right) (amplified, not in scale). (a) CST model; (b) prototype.

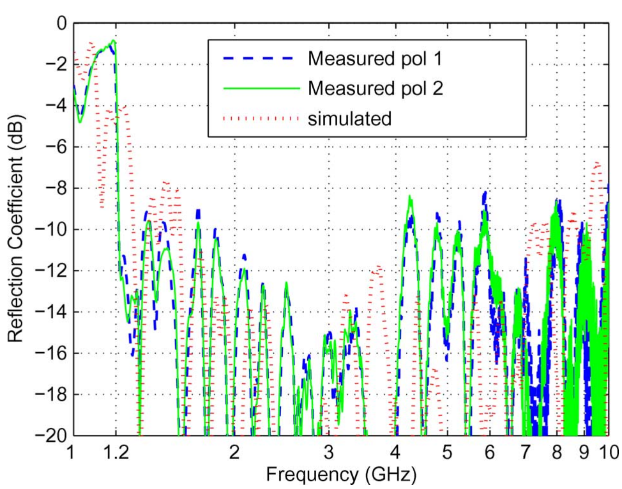

Fig. 11. Simulated and measured reflection coefficients of the compact 1.2–10 GHz Eleven feed at the ports of the center puck circuit board with a 50-Ohm reference port impedance.

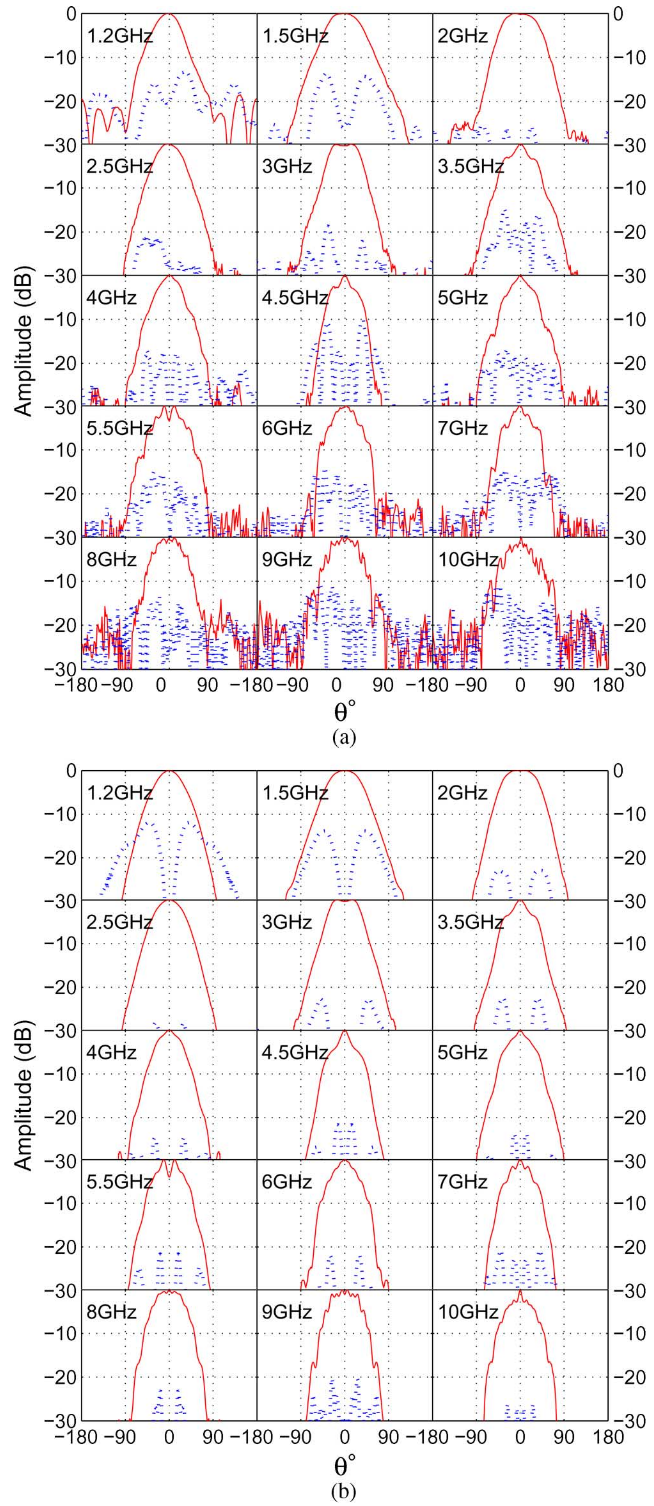

Fig. 12. Measured co(solid)- and cross(dashed)-polar radiation patterns at 15 frequencies in $\varphi = 45^\circ$ plane of the 1.2–10 GHz Eleven antenna. The upper graph shows the patterns of the total radiation field, and the lower graph of the BOR_1 components of the field.

gives a nearly optimal G/T value for the Eleven feed [13]. From the figure, it can be seen that the simulated and measured results agree with each other quite well. The aperture efficiency e_{ap} is better than -3 dB over 1.2–10 GHz. The spillover efficiency e_{sp} is better than -0.4 dB over the most part of the frequency band but degraded to about -0.7 dB at both the low and high frequency ends. The reason for the e_{sp} degradation at the low frequency end is probably the effect of the re-arrangement of the last three dipoles, as shown in Fig. 9. The degradation of e_{sp} at high frequencies is due to the increase of the higher modes of φ variation. The BOR_1 efficiency e_{BOR1} is almost higher than -0.5 dB over the whole band. The polarization efficiency e_{pol} and the phase efficiency e_ϕ are very high (better than -0.1 dB), except for the low frequency end, again due to the re-arrangement of the dipoles. The illumination efficiency e_{ill} is almost constant due to the constant beamwidth.

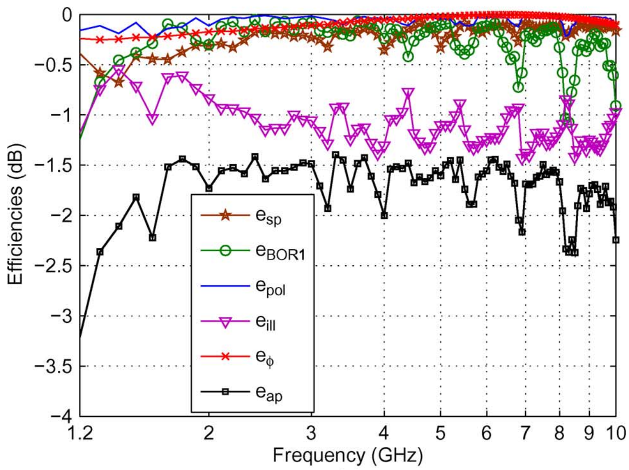

(a)

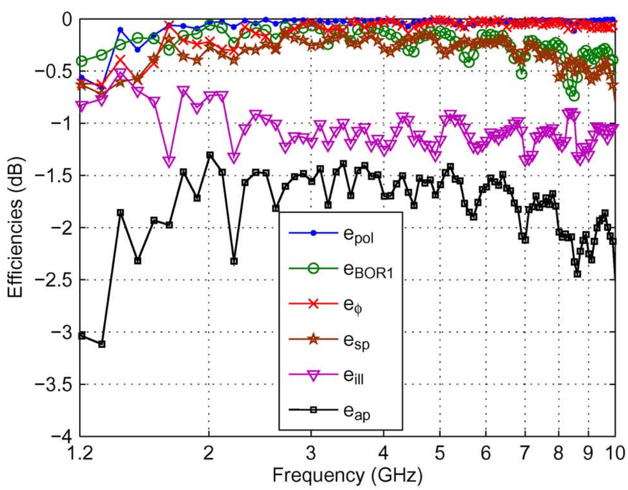

(b)

Fig. 13. Calculated aperture efficiency and its sub-efficiencies of the 1.2–10 GHz Eleven feed for a reflector with subtended angle of $2 \times 60^{\circ}$. Results are based on (a) simulated and (b) measured complex far-field functions. Center blockage is neglected.

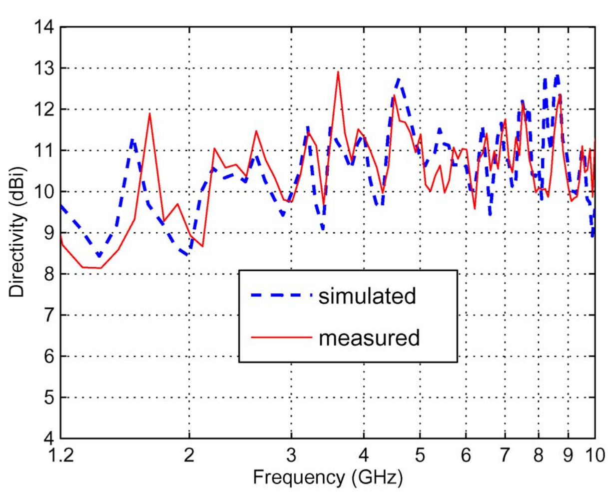

Fig. 14. Simulated and measured directivity of the 1.2–10 GHz Eleven antenna.

Fig. 14 shows the simulated and measured directivity of the Eleven feed with good agreement. It is observed that both the directivity and the aperture efficiency have a certain fluctuation over the frequency band, which is a characteristic of log-periodic array antennas. The directivity of the whole reflector antenna will also have a less-than-1 dB fluctuation due to the fluctuation of the aperture efficiency. This fluctuation can be calibrated out by proper calibration procedures [26].

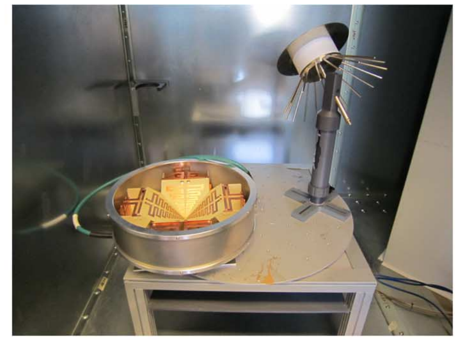

(a)

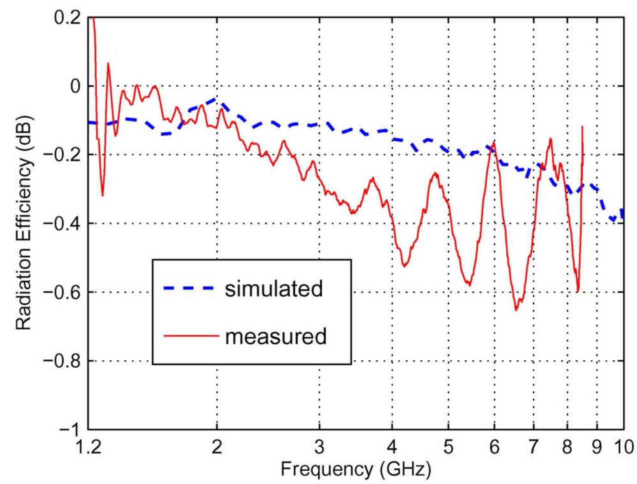

(b)

Fig. 15. Simulated and measured radiation efficiency of the 1.2–10 GHz Eleven antenna by using CST MWS and Bluetest reverberation chamber, respectively. (a) Set-up in bluetest reverberation chamber; (b) simulated and measured data.

Fig. 15 shows the simulated and measured radiation efficiency of the Eleven antenna. Radiation efficiency e_{rad} measures the ohmic losses of an antenna, which is a critical characteristic for feeds used in radio telescopes. The measurement was carried out over 1.2–8.5 GHz, by using the Bluetest reverberation chamber [27], [28], including the hybrids and combiners. But the results shown in Fig. 15 are only for the Eleven feed with the center puck circuit board, where the measured data are obtained by removing the ohmic loss in the feeding network (the hybrids and combiner), using a rigorous calibration method presented in [29]. The reason for the measured frequency range of only 1.2–8.5 GHz is the present limitations of the chamber above 8.5 GHz. From both the simulated and measured data, it is seen that the radiation efficiency (ohmic loss) of the Eleven feed is between -0.1 dB and -0.4 dB over 1.2–8.5 GHz. The fluctuation of the measured curve, particularly at both the low frequency end and above 3.5 GHz, is due to the measurement error in the reverberation chamber [27].

VII. Conclusion

By re-arranging the outermost three folded dipoles, a compact 1.2–10 GHz Eleven feed has been developed. The volume of the new design has only 40% of the original, with a very similar performance. Thus, the same compact cryostat for 2–13 GHz Eleven feed can be used for the 1.2–10 GHz feed system. By doing so, the blockage due to the feed system is minimized, and the capacity requirement for cryogenic cooling system (therefore the power consumption) is reduced significantly.

Acknowledgment

The authors would like to thank B. Klein for his comments on the manuscript.

References

[1] J. D. Kraus and R. J. Marhefka, *Antennas for All Applications*. Berlin, Germany: Springer, 2003.
[2] A. Niell, A. Whitney, W. Petrachenko, W. Schlüter, N. Vandenberg, H. Hase, Y. Koyama, C. Ma, H. Schuh, and G. Tuccari, (2005) VLBI2010: Current and Future Requirements for Geodetic VLBI Systems IVS WG3 Rep. [Online]. Available: http://ivscc.gsfc.nasa.gov/about/wg/wg3
[3] Y. Yan, J. Zhang, Z. Chen, W. Wang, F. Liu, and L. Geng, "Progress on Chinese spectral radioheliograph—CSRH construction," in *2011 XXX URSI GASS*, Istanbul, Turkey, Aug. 13–20, 2011.
[4] P. Hall, *The SKA: An Engineering Perspective*. Berlin, Germany: Springer, 2005.
[5] V. Rodriguez, "An open-boundary quad-ridged guide horn antenna for use as a source in antenna pattern measurement anechoic chamber," *IEEE Antennas Propogat. Mag.*, vol. 48, no. 2, pp. 157–160, Apr. 2006.
[6] A. Akgiray, S. Weinreb, and W. Imbriale, "Design and measurements of dual-polarized wideband constant-beamwidth quadruple-ridged flared horn," in *2011 IEEE AP-S International Symp. on Antennas Propag.*, Spokane, WA, Jul. 3–8, 2011.
[7] R. Gawande and R. Bradley, "Towards an ultra wideband low noise active sinuous feed for next generation radio telescopes," *IEEE Trans. Antennas Propagt.*, vol. 59, no. 6, pp. 1945–1953, Jun. 2011.
[8] G. Cortes-Medellin, "Non-planar quasi-self-complementary ultra-wideband feed antenna," *IEEE Trans. Antennas Propogat.*, vol. 59, no. 6, pp. 1935–1944, Jun. 2011.
[9] J. Yang, S. Pivnenko, and P.-S. Kildal, "Comparison of two decade-bandwidth feeds for reflector antennas: Eleven antenna and quadridge horn," in *Fourth Eur. Conf. Antennas and Propagation (EuCAP 2010)*, Barcelona, Spain, Apr. 12–16, 2010.
[10] R. Olsson, P.-S. Kildal, and S. Weinreb, "The Eleven antenna: A compact low-profile decade bandwidth dual polarized feed for reflector antennas," *IEEE Trans. Antennas Propogat.*, vol. 54, no. 2, pp. 368–375, Feb. 2006.
[11] P.-S. Kildal, R. Olsson, and J. Yang, "Development of three models of the Eleven antenna: A new decade bandwidth high performance feed for reflectors," in *1st Eur. Conf. Antennas Propagat. (EuCAP2006)*, Nice, France, Nov. 6–10, 2006.
[12] J. Yang, X. Chen, N. Wadefalk, and P.-S. Kildal, "Design and realization of a linearly polarized Eleven feed for 1–10 GHz," *IEEE Antennas Wireless Propagat. Lett.*, vol. 8, pp. 64–68, 2009.
[13] J. Yang, M. Pantaleev, P.-S. Kildal, B. Klein, Y. Karandikar, L. Helldner, N. Wadefalk, and C. Beaudoin, "Cryogenic 2–13 GHz Eleven feed for reflector antennas in future wideband radio telescopes," *IEEE Trans. Antennas Propagat.*, vol. 59, no. 6, pp. 1918–1934, Jun. 2011.
[14] J. Yin, J. A. Aas, J. Yang, and P.-S. Kildal, "Monopulse tracking performance of multi-port Eleven antenna for use in terminals for satellite communications," in *Second Eur. Conf. Antennas and Propagation (EuCAP 2007)*, Edinburgh, Nov. 11–16, 2007.
[15] J. Yang, S. Pivnenkoy, T. Laitinenz, J. Carlsson, and X. Chen, "Measurements of diversity gain and radiation efficiency of the Eleven antenna by using different measurement techniques," in *4th Eur. Conf. Antennas Propagat. (EuCAP2010)*, Barcelona, Spain, Apr. 12–16, 2010.
[16] X. Chen, P.-S. Kildal, J. Carlsson, and J. Yang, "Comparison of ergodic capacities from wideband MIMO antenna measurements in reverberation chamber and anechoic chamber," *IEEE Antennas Wireless Propagat. Lett.*, vol. 10, pp. 446–449, 2011.
[17] R. Wang and J. Yang, "A new compact antenna for digital television reception based on the eleven antenna," *Microw. Opt. Technol. Lett.*, 2011, accepted for publication.
[18] A. Yasin, J. Yang, and T. Ostling, "A novel compact dual band feed for reflector antennas based on choke horn and circular Eleven antenna," *IEEE Trans. Antennas Propogaat.*, vol. 57, no. 10, pp. 3300–3302, Oct. 2009.
[19] P. J. Hall, "Power considerations for the square kilometre array (SKA) radio telescope," in *Proc. 2011 XXX URSI GASS*, Istanbul, Aug. 13–20, 2011.
[20] J. Yang, D. Nyberg, and J. Yin, "Impedance matrix of a folded dipole pair under Eleven configuration," *IET Microw. Antennas Propagat.*, vol. 4, no. 6, pp. 697–703, June 2010.
[21] J. Yang, "On conditions for constant radiation characteristics for log-periodic array antennas," *IEEE Trans. Antennas Propagat.*, vol. 58, no. 5, pp. 1521–1526, May 2010.
[22] CST Microwave Studio, 3D EM Simulation software [Online]. Available: www.cst.com
[23] P.-S. Kildal and Z. Sipus, "Classification of rotationally symmetric antennas as types BOR_0 and BOR_1," *IEEE Antennas Propagat. Mag.*, vol. 37, no. 6, pp. 114–117, Dec. 1995.
[24] M. Denstedt, T. Ostling, J. Yang, and P.-S. Kildal, "Tripling bandwidth of hat feed by genetic algorithm optimization," in *IEEE 2007 Int. Symp. Antennas and Propagation*, Honolulu, Hawai, Jun. 10–15, 2007.
[25] J. Yang and P.-S. Kildal, "Optimization of reflection coefficient of large log-periodic array by computing only a small part of it," *IEEE Trans. Antennas Propagat.*, vol. 59, no. 6, pp. 1790–1797, Jun. 2011.
[26] O. M. Smirnov, "Revisiting the radio interferometer measurement equation. II. Calibration and direction-dependent effects," *Astronomy Astrophys.*, Jan. 5, 2011, accepted for publication.
[27] K. Rosengren and P.-S. Kildal, "Radiation efficiency, correlation, diversity gain, and capacity of a six monopole antenna array for a MIMO system: Theory, simulation and measurement in reverberation chamber," *Proc. Inst. Electr. Eng, Microw. Antennas Propagat.*, vol. 152, no. 1, pp. 7–16, February 2005.
[28] Bluetest AB [Online]. Available: http://www.bluetest.se
[29] H. Raza, J. Yang, and A. Hussain, "Measurement of radiation efficiency of multiport antennas with feeding network corrections," *IEEE Antennas Wireless Propag. Lett.*, vol. 11, pp. 89–92, 2012.

Jian Yang (M'02–SM'10) received the B.S. degree from the Nanjing University of Science and Technology, Nanjing, China, in 1982, and the M.S. degree from the Nanjing Research Center of Electronic Engineering, Nanjing, China, in 1985, both in electrical engineering, and the Swedish Licentiate and Ph.D. degrees from the Chalmers University of Technology, Gothenberg, Sweden, in 1998 and 2001, respectively.

From 1985 to 1996, he was with the Nanjing Research Institute of Electronics Technology, Nanjing, China, as a Senior Engineer. From 1999 to 2005, he was with the Department of Electromagnetics, Chalmers University of Technology as a Research Engineer. During 2005 and 2006, he was with COMHAT AB as a Senior Engineer. From 2006, he has been an Assistant Professor at the Department of Signals and Systems, Chalmers University of Technology. From 2010, he has been titled as Associate Professor. His research interests include ultra-wideband antennas and UWB feeds for reflector antennas, UWB radar systems, UWB antennas in near-field sensing applications, hat-fed antennas, reflector antennas, radome design, and computational electromagnetics.

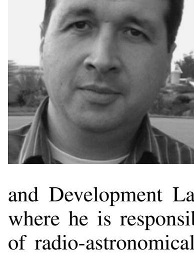

Miroslav Pantaleev received the M.S. degree in electrical engineering from the Technical University of Sofia, Sofia, Bulgaria, in 1995, and the M.S. and Ph.D. degrees from the Chalmers University of Technology, Gothenberg, Sweden, in 2000 and 2006, respectively.

During his doctoral studies, he was involved in beam measurement characterization for HIFI Instrument of Herschel satellite and later in the design and tests of the HEB mixer for the APEX telescope. He is currently the Head of the Operation and Development Laboratory, Onsala Space Observatory, Onsala, Sweden, where he is responsible for design, integration, implementation, and testing of radio-astronomical equipment. His main areas of research are low noise cryogenic amplifiers and mixers, system integration of optical, cryogenic and mechanical components, and cryogenic techniques for laboratory applications.

Per-Simon Kildal (M'82–SM'84–F'95) has been a Professor at Chalmers University of Technology, Gothenburg, Sweden, since 1989. He has authored an antenna textbook, and more than 100 journal articles and letters in IEEE or IET journals. He has designed two very large antennas, including the Gregorian dual-reflector feed of the Arecibo radiotelescope. He has invented several reflector antenna feeds, the latest being the so-called "Eleven antenna." He is the originator of the concept of soft and hard surfaces, recently resulting in the gap waveguide, a new low-loss metamaterials-based transmission line advantageous mainly above 30 GHz. His research group has pioneered the reverberation chamber into an accurate measurement tool for antennas and wireless terminals subject to Rayleigh fading.

Prof. Kildal received two best paper awards for articles published in the IEEE TRANSACTIONS ON ANTENNAS AND PROPAGATION, and he is the recipient of the 2011 Distinguished Achievements Award of the IEEE Antennas and Propagation Society.

Leif Helldner has been a Research Engineer in the Operation and Development Laboratory at Onsala Space Observatory, Onsala, Sweden, since 1989. For more than 20 years he has been working with development, test and maintenance of front-end and back-end electronics for radio astronomy. He has excellent experience in design and test of RF, IF, automatization and digital electronics, mechanical and cryogenic systems for radio astronomy. He has been involved in developing hardware systems for SEST, APEX, ALMA, and the Onsala telescopes and radiometers, and was the project manager for the construction of a LOFAR station in Sweden. His interests are mechanical and cryogenic design, and international VLBI and LOFAR technical activities.